Enhancement of Fe magnetic moments in ferromagnetic $Fe_{16}N_2$

B. I. Min
Department of Physics and Center for Advanced Materials Physics, Pohang Institute of Science and Technology, Pohang, Kyungbuk 790-600, Korea
(Received 17 December 1991)

In order to investigate the electronic and magnetic properties of an $Fe_{16}N_2$ ferromagnet, we have performed electronic-structure calculations employing the total-energy self-consistent local-density-functional linearized muffin-tin orbital band method. Band structures, density of states, Stoner parameters, magnetic moments, and cohesive bonding properties for paramagnetic or ferromagnetic $Fe_{16}N_2$ are obtained. The effect of spin-orbit interaction on the magnetism is also explored. Based on these results, the magnetic structure and the microscopic origin of the enhancement of Fe magnetic moments in this compound are investigated. Magnetic moments of three types of Fe [Fe(I), Fe(II), and Fe(III)] in $Fe_{16}N_2$ are 2.13, 2.50, and 2.85μ_B, respectively. Large enhancement of the magnetic moment is observed in Fe(II) and Fe(III), which are located farther from N than Fe(I). This suggests that the local environment plays a very important role in determining the Fe magnetic moments in this compound. The orbital contribution to the magnetic moment in Fe atoms is minor, a total of 0.56μ_B in the unit cell. Our value of the average magnetic moment per Fe atom, 2.50μ_B, is a bit smaller than the reported value, $\sim$3.0μ_B, estimated from the experiment.

I. INTRODUCTION

In the early 1970's, Kim and Takahashi[1] observed a giant saturated magnetic moment in the Fe film deposited in a nitrogen atmosphere and interpreted that this large magnetization came from $Fe_{16}N_2$, which is formed in the Fe-N film. Assuming that the Fe-N film is a polycrystal, composed of α-Fe and $Fe_{16}N_2$, they have deduced the average magnetic moment of the Fe atom, 3.0μ_B, from the measured value of the saturated magnetic flux density of the film (B_s), 2.58 T. This magnetic moment is much larger than that of bcc α-Fe, 2.22μ_B (saturated magnetic flux density of bcc α-Fe is about 2.2 T). Since a large saturated magnetic flux density is an important factor for the application to advanced magnetic materials, extensive research has been carried out on $Fe_{16}N_2$. Reproduction of the single-phase sample has not been successful, however.

Recently, Komuro *et al.*[2] successfully made a single-crystal Fe-N film of $Fe_{16}N_2$, which was epitaxially grown on the substrate of Fe/GaAs(100) using molecular beam epitaxy (MBE). They reported that the saturated magnetic flux density of the sample is 2.8–3.0 T, the largest among the magnetic materials available so far (the corresponding average magnetic moment per Fe atom is 3.1–3.3μ_B). Other groups[3,4] have also reported similar results on this material, which confirmed the result of Kim and Takahashi.[1] From a measurement of the Mössbauer spectrum, Nakajima *et al.*[4] obtained the magnetic moments of 1.3, 2.5, and 3.8μ_B for the three types of Fe atoms in $Fe_{16}N_2$, respectively. Hence, the first-nearest-neighbor Fe atom of N [Fe(I)] yields the smallest moment while Fe(III), which is located the farthest from the N atom, yields the maximum moment which is much enhanced from the value of α-Fe. However, the average magnetic moment per Fe atom in this case is only 2.53μ_B, which is smaller than the estimate made by Kim and Takahashi[1] or Komuro *et al.*[2]

Sakuma[5] investigated systematically the electronic and magnetic structures for a series of iron nitrides, Fe_3N, Fe_4N, $Fe_8N(=Fe_{16}N_2)$ using the LMTO (linearized muffin-tin orbital) band method.[6] He has explored the effects of the interstitial N atom and its concentration on the magnetic and electronic structures of these compounds. He found that the lower N concentration gives the larger magnetic moments with the exception of $Fe_{16}N_2$. In $Fe_{16}N_2$, he obtained 2.40μ_B for the average magnetic moment per Fe atom, which is larger than that of bcc α-Fe. However, this value is smaller than the experimental estimate, $\sim$3.0μ_B.

In this study, we have carried out the total-energy electronic structure calculations in order to understand the microscopic origin of the enhancement of the Fe magnetic moments in $Fe_{16}N_2$. We have investigated the effect of interactions between the *d* band of the Fe atoms and the *s,p* band of the N atom and also the interactions between Fe-Fe on the magnetization. We have calculated the total energies of paramagnetic and ferromagnetic $Fe_{16}N_2$ to examine the cohesive bonding properties in this compound. The effect of the spin-orbit interaction on the magnetic moments is also discussed.

The self-consistent local-density-functional[7] LMTO band method is employed and the tetrahedron method for the Brillouin-zone integration and the form of von Barth–Hedin for the exchange-correlation potential is utilized. An orbital contribution to the magnetic moment is obtained by including the spin-orbit interaction in a perturbative way.[8] In this way, both the magnetic exchange-correlation interaction and the spin-orbit interaction are taken into account simultaneously in the self-consistent variational step.

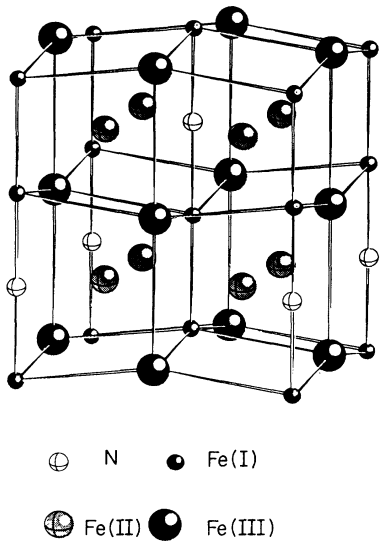

FIG. 1. Crystal structure of $Fe_{16}N_2$.

II. CRYSTAL STRUCTURE

The basic structure of $Fe_{16}N_2$ (α'' phase) comprises eight ($2\times2\times2$) bcc Fe unit cells in which two N atoms are located between two Fe [Fe(I)] atoms along the z axis (see Fig. 1). The Bond length of Fe(I)-Fe(I), which includes the N atom in the middle, increases while the bond length of Fe(I)-Fe(I), which does not have the N atom, decreases so that xy planes are deformed alternatively along the z direction to possess a puckering structure. As seen in Fig. 2, $Fe_{16}N_2$ crystallizes in the body-centered tetragonal (bct) and the space group is D_{4h}^{17}, which is symorphic.[9] In the primitive bct unit cell, there is one formula unit (Fe_8N) with nine atoms, one type of N atom, and three types of eight Fe atoms [two Fe(I), four Fe(II), two Fe(III)].

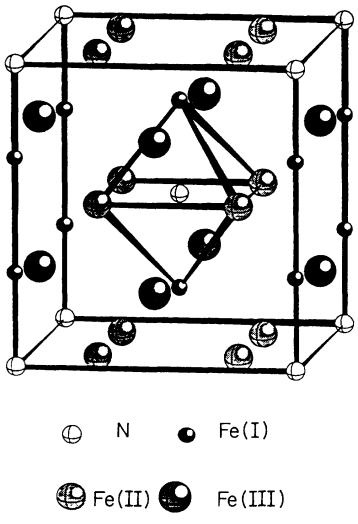

FIG. 2. Body-centered tetragonal (bct) unit cell of $Fe_{16}N_2$. Lattice constants of the a and c axes are 5.72 and 6.29 Å, respectively.

TABLE I. Atomic positions in $Fe_{16}N_2$ bct unit cell, in units of primitive lattice vectors.

N	1	(0.00,0.00,0.00)
Fe(I)	2	(0.00,0.00,0.31)(0.50,0.50,0.19)
Fe(II)	4	(0.25,0.25,0.00)(0.75,0.25,0.00)
		(0.25,0.75,0.00)(0.75,0.75,0.00)
Fe(III)	2	(0.00,0.50,0.25)(0.50,0.00,0.25)

The positions of each atom in the unit cell are given in Table I. The atom is situated at the deformed octahedral interstitial site surrounded by six Fe atoms. The distance from N to Fe(I) in the z direction is a little bit shorter than the distance to Fe(II) in the xy plane. The Fe(III) atom is located farthest from the N atom. Fe(III) is at the center of the tetragonal structure made of eight nearest-neighbor Fe(II) atoms. Thus, the local environment of the Fe(III) atoms is similar to the case of bcc α-Fe, except that the nearest-neighbor distance is longer.

III. ELECTRONIC STRUCTURE OF PARAMAGNETIC $Fe_{16}N_2$

The total density of states (DOS) and site-projected local DOS (LDOS) in the paramagnetic phase of $Fe_{16}N_2$ at the experimental lattice constant are given in Figs. 3 and 4, respectively. A high DOS at the Fermi level (E_F) [$N(E_F)=30.3$ states/eV] in Fig. 3 originates mostly from the d band of Fe atoms and predicts possible magnetic or structural phase transitions. In fact, we obtained the Stoner parameter, $S=1.8$ [$S=N(E_F)I_{xc}$; I_{xc} equals the intra-atomic exchange-correlation integral], which is larger than 1.0 and so induces the ferromagnetic instability as in the case of α-Fe.

As seen in Fig. 4, Fe(III), which is the farthest from the N atom, has the highest LDOS at E_F, while Fe(I), which is closest to N, has the lowest LDOS. Hence, the ferromagnetic instability and the corresponding magnetic moment are expected to be the largest in Fe(III). This is attributed to the fact that hybridization interaction with neighboring N atoms becomes larger with a reduced distance in Fe(I) and, accordingly, the bandwidth becomes larger.

The narrow DOS located $\sim$15 eV below E_F is mostly

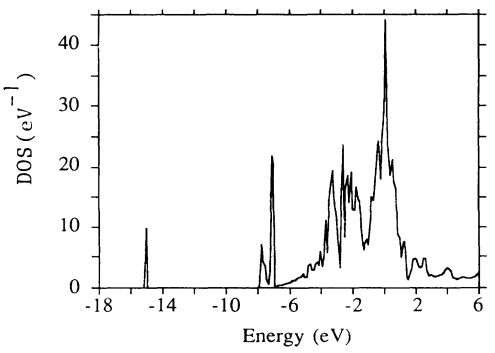

FIG. 3. Total density of states (DOS per unit cell in unit of states/eV) of paramagnetic $Fe_{16}N_2$.

TABLE II. Angular momentum and site-projected local DOS at E_F, $N_l(E_F)$ in units of states/Ry, and charge occupancies, Q_l, of paramagnetic $Fe_{16}N_2$.

	N_s	N_p	N_d	$N_{tot}(E_F)$
	Q_s	Q_p	Q_d	Q_{tot}
N	2.45	1.22		3.67
	1.68	3.85		5.53
Fe(I)	0.15	0.58	27.16	27.89
	0.61	0.81	6.57	7.99
Fe(II)	0.25	0.49	53.34	54.08
	0.59	0.72	6.59	7.90
Fe(III)	0.14	0.47	67.46	68.07
	0.66	0.64	6.64	7.94

due to the s band of the N atom in which a bit of band states of Fe(I) and Fe(II) are also mixed. Two sharp DOS peaks located 7–8 eV below E_F correspond to the hybridized states between the p band of N and the bands of Fe(I) and Fe(II). The smaller peak on the left possesses relatively more s-band character of Fe while the one on the right possesses more d-band character. The high DOS in the wide range of -4–2 eV originates from the d bands of three types of Fe with which some of the N p-band states are also hybridized. Table II provides the LDOS at E_F and the numbers of occupied electrons per each atom.

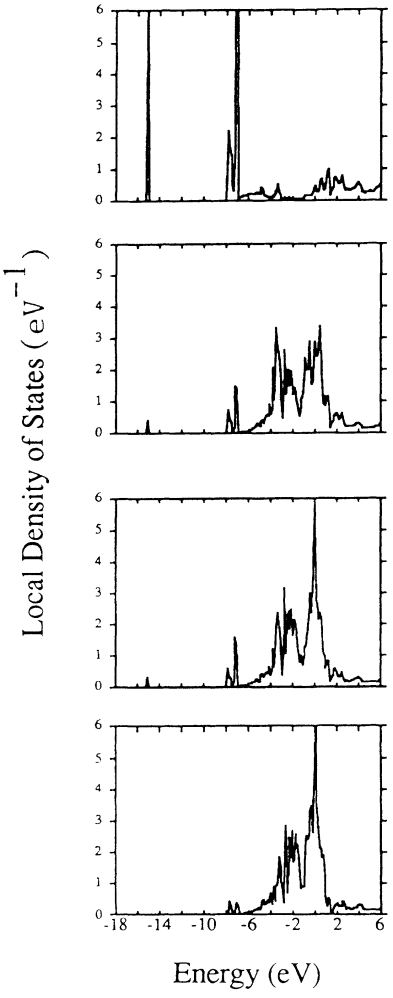

FIG. 4. Site-projected local density of states (LDOS in unit of states/eV) of paramagnetic $Fe_{16}N_2$. Panels from the top correspond to the local DOS of N, Fe(I), Fe(II), and Fe(III), respectively.

IV. ELECTRONIC STRUCTURE OF FERROMAGNETIC $Fe_{16}N_2$

The total density of states and site-projected local DOS in the ferromagnetic phase of $Fe_{16}N_2$ are given in Figs. 5 and 6, respectively. Due to the exchange splitting between spin-up and spin-down band states, the total DOS at E_F (6.26 states/eV) is only about 20% of that of the paramagnetic phase, which allows a stable ferromagnetic ground state. The magnitude of the exchange energy splitting is the largest in Fe(III), which has the highest LDOS at E_F in the paramagnetic phase, and so is the magnetic moment. Compared to the almost filled spin-up d band of Fe(III), about 0.3 electron states are empty in the spin-up d band of Fe(I). Smaller exchange splitting in Fe(I) than in Fe(III) gives rise to the shift up in energy for the spin-up band and the shift down for the spin-down band, and so about 0.3 electrons transfer from the spin-up to the spin-down band to reduce the magnetic moment.

Table III presents the numbers of the occupied electrons per each atom. We obtain magnetic moments, 2.13, 2.50, and 2.85μ_B, for Fe(I), Fe(II), and Fe(III), respectively. The enhancement is prominent in Fe(II) and Fe(III), whose magnetic moments are increased much from that of bcc α-Fe, 2.22μ_B. The average magnetic moment of the above three types of Fe is 2.50μ_B, which is a little bit larger than that of Sakuma[5] (2.43μ_B), but still smaller than the experimental estimate ($\sim$3.0μ_B). Sakuma obtained the magnetic moments, 2.27, 2.25, and 2.83μ_B for Fe(I), Fe(II), and Fe(III), respectively. The main difference from ours is the size of the magnetic moments in Fe(I) and Fe(II) Sakuma obtained similar magnitudes of magnetic moments for Fe(I) and Fe(II), whereas we get a much larger value for Fe(II). Of course, the size of magnetic moments will depend on the atomic sphere ra-

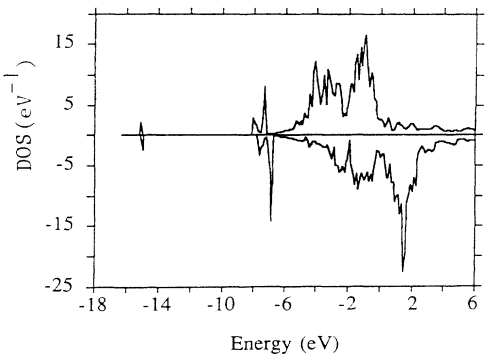

FIG. 5. Total density of states (DOS per unit cell in unit of states/eV) of ferromagnetic $Fe_{16}N_2$.

TABLE III. Angular momentum and site-projected occupancies, Q_l, of ferromagnetic $Fe_{16}N_2$. ↑ and ↓ denote spin-up and spin-down electrons, respectively. Local density of states at E_F, $N(E_F)$ in units of states/Ry, are also provided.

		Q_s	Q_p	Q_d	Q_{tot}	$N(E_F)$
N	↑	0.87	1.94		2.81	2.46
	↓	0.82	1.92		2.75	0.43
Fe(I)	↑	0.30	0.40	4.37	5.07	6.10
	↓	0.31	0.44	2.18	2.94	7.23
Fe(II)	↑	0.30	0.35	4.55	5.20	4.27
	↓	0.31	0.38	2.01	2.70	5.93
Fe(III)	↑	0.33	0.31	4.74	5.38	1.51
	↓	0.34	0.36	1.83	2.53	5.88

dii used in the LMTO band calculation. We used the same sphere radius (2.64 a.u.) for both N and Fe atoms, whereas Sakuma used the sphere radii, 1.70 and 2.72 a.u. for the N and Fe atoms, respectively. In order to examine the effect of the atomic sphere radius on the magnetic moment, we have performed another band calculation with the same sphere radii used by Sakuma. We have again obtained the enhanced magnetic moments for Fe(II), Fe(III) (2.41 and $2.97\mu_B$) and the smaller one for Fe(I) ($2.05\mu_B$), which are similar to our former results within 5%. Since local environments for the two Fe atoms are quite different, it is more likely that the magnetic moments of the two atoms also become different. Evidently, a stronger hybridization interaction with the N atom in Fe(I) will give rise to a smaller magnetic moment than in Fe(II). The enhancement of the magnetic moment in Fe(III) is ascribed to the d-band localization occurring in consequence of a relatively longer bond length to the near-neighbor Fe atoms than in bcc α-Fe. The distance to the nearest neighbor, Fe(II), is 4% longer than that in bcc α-Fe. On the other hand, the d band in Fe(I) becomes rather delocalized due to the hybridization interaction with the nearest-neighbor N atom and due to a shorter near-neighbor distance to Fe(II) (5% shorter than in bcc α-Fe) as well, Thus, the magnetic moment in Fe(I) is reduced compared to bcc α-Fe. However, the reduction here is not as large as in the $Fe_{16}B_2$, $Fe_{16}C_2$, or Fe-Al systems in which hybridization interaction with B, C, or Al reduces the magnetic moment of Fe a lot.[10,11] The magnetic moment of Fe(I) in $Fe_{16}B_2$ and $Fe_{16}C_2$ becomes 1.96 and $2.03\mu_B$, respectively.[10] The Fe(II) atom has an intermediate value between Fe(I) and Fe(III). Influence by the magnetic moments of near-neighbor Fe atoms, the magnetic moment of the N atom also polarizes in the same direction with a magnitude of $0.06\mu_B$. Therefore, the total magnetic moment in the unit cell is $20\mu_B$, which corresponds to the magnetic flux density of ~2.3 T. This value is smaller than the experimental values, 2.8–3.0 T.[1,2]

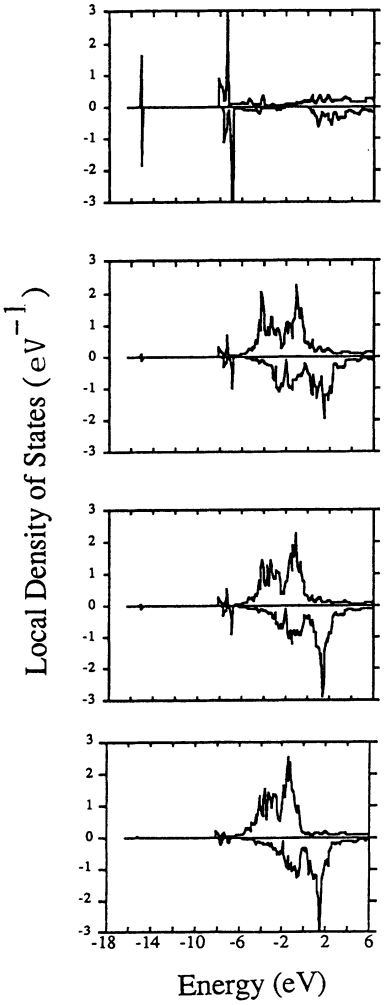

FIG. 6. Site-projected local density of states (LDOS in unit of states/eV) of ferromagnetic $Fe_{16}N_2$. Panels from the top correspond to the LDOS of N, Fe(I), Fe(II), and Fe(III), respectively. In each panel, the upper part is spin-up LDOS and lower part is spin-down LDOS.

Orbital polarizations in $Fe_{16}N_2$ stemming from the spin-orbit interaction is non-negligible. However, the value is not large enough to compensate the difference between the theory and the experiment. Orbital magnetic moments, 0.06, 0.07, and $0.08\mu_B$, are obtained for Fe(I), Fe(II), and Fe(III), respectively, and so the total orbital magnetic moment in the unit cell is $0.56\mu_B$. Moreover, introducing the spin-orbit interaction reduces the spin polarization in each Fe atom slightly and thus the increase of the total magnetic moment in the unit cell is minor.

V. DISCUSSIONS AND CONCLUSION

The average magnetic moment per Fe atom in our calculation, $2.50\mu_B$, is smaller than the value estimated from the measurement, $\sim 3.0\mu_B$. The origin of the difference between the theory and the experiment can be analyzed in three respects.

The first possibility is that the local-density-functional approach employed in our study could be inappropriate in describing the electronic and magnetic structures of $Fe_{16}N_2$. This is always possible since the description of local-density approximation (LDA) is known to be poor for the compound with strong local bonding. Experiences, however, indicate that LDA descriptions for electronic and magnetic structures in transition-metal com-

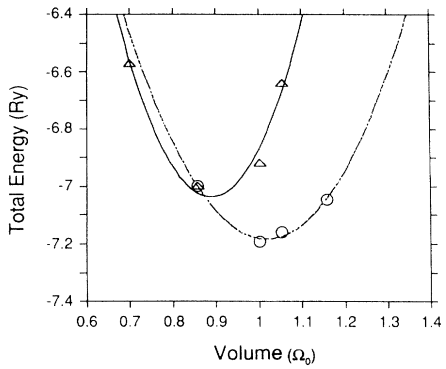

FIG. 7. Total energy of paramagnetic (marked by triangle) and ferromagnetic (marked by circle) $Fe_{16}N_2$ vs volume. The volume is renormalized by the experimental volume (Ω_0) and the reference value of the total energy of -20430 Ry.

pounds are not so bad. In order to test the validity of the LDA description for the cohesive bonding properties in this compound, we performed total-energy electronic structure calculations as varying the lattice constant of $Fe_{16}N_2$. Figure 7 provides total energy versus volume for both the paramagnetic and ferromagnetic $Fe_{16}N_2$. The equilibrium volume for the paramagnetic phase is too small, $0.89\Omega_0$ (Ω_0 is the experimental volume). As spin polarization is introduced, volume expansion occurs and the total energy is lowered. The energy gain of the ferromagnetic phase is about 44 mRy and the equilibrium volume is $1.02\Omega_0$, which is very close to the experiment. This good agreement reveals that the cohesive bonding properties in $Fe_{16}N_2$ are fairly well described by the LDA. As the volume increases, the magnetic moment increases. The average magnetic moments per Fe atom become 2.59 and $2.69\mu_B$ for volume expansions of 5 and 16%, respectively. On the other hand, the magnetic moment decreases rapidly as the volume is reduced. At about 15% reduction of volume, the ferromagnetic phase becomes unstable and the magnetic moment vanishes.

The second possibility is the enhancement of the magnetic moment at the surface. It is well known that the magnetic moment is greatly enhanced at the surface of the film. For example, enhancements of magnetic moment at the surfaces of Fe(001) and Fe(110) are predicted to be 35 and 20%, respectively, with respect to their bulk values.[12] Hence, surface electronic and magnetic studies for this material may be essential to resolve the problem.

The third possible reason may lie in the experiment. There may be another impurity phase in the film sample which has a larger magnetic moment besides α-Fe and $Fe_{16}N_2$, different from the assumption by Kim and Takahashi.[1] In fact, Nakajima and Okamoto[3] reported that the α' martensite phase (FeN) is observed in their Fe-N sample which is prepared by the N-ion implantation. Furthermore, Mössbauer studies by Nakajima *et al.*[4] yield the average magnetic moment per Fe atom, $2.53\mu_B$, which is smaller than the estimate by Kim and Takahashi[1] and Komuro *et al.*[2] Thus, refined measurements are also necessary for determining more precise magnetic moments.

In summary, based on the electronic structures of $Fe_{16}N_2$, the magnetic structures and the enhancement of the magnetic moment in Fe atoms are investigated. Total-energy calculations reveal that the cohesive bonding properties in this compound are well described by the local-density approximation. Spin magnetic moments for three types of Fe, Fe(I), Fe(II), and Fe(III), are 2.13 , 2.50, and $2.85\mu_B$, respectively, and the orbital contribution to magnetic moments is estimate to be minor. Thus, large enhancements of the magnetic moment are found in Fe(II) and Fe(III), which are located far from the N atom. In the case of Fe(I), the magnetic moment less than in bcc α-Fe is caused by the d-band delocalization, which is induced by the strong hybridization interaction with nearest-neighbor N atom and also by the shorter bond length to near-neighbor Fe atoms. In contrast, the d band in Fe(III) is rather localized due to the longer bond lengths between Fe atoms and leads to the enhancement of magnetic moment. The above result implies that the local environment plays an important role in determining the magnetic moments of Fe atoms in this compound.

ACKNOWLEDGMENTS

Helpful discussions with C. S. Kim, J. I. Lee, and S. C. Hong are greatly appreciated. This work was supported by CAMP at POSTECH and CTP at SNU.

[1]T. K. Kim and M. Takahashi, Appl. Phys. Lett. **20**, 492 (1972).
[2]M. Komuro, Y. Kozono, M. Hanazono, and Y. Sugita, J. Appl. Phys. **67**, 9 (1990); J. Magn. Soc. Jpn. **14**, 701 (1990).
[3]K. Nakajima, S. Okamoto, and T. Okata, J. Appl. Phys. **65**, 1 (1989); K. Nakajima and S. Okamoto, Appl. Phys. Lett. **54**, 19 (1990); **56**, 92 (1990); J. Magn. Soc. Jpn. **14**, 271 (1990).
[4]K. Nakajima, and S. Okamoto, M. Takata, and H. Sekizawa, J. Magn. Soc. Jpn. **15**, 703 (1991); see also the special issue of J. Magn. Soc. Jpn. **15**. No. 3 (1991).
[5]A. Sakuma, J. Phys. Soc. Jpn. **60**, 2007 (1991); J. Magn. Magn. Mater. **102**, 127 (1991).
[6]O. K. Andersen, Phys. Rev. B **12**, 3060 (1975); H. L. Skriver, *The LMTO Method,* Springer Series in Solid State Sciences Vol. **41**, (Springer-Verlag, Berlin, 1984).
[7]P. Hohenberg and W. Kohn, Phys. Rev. **136**, B864 (1964); W. Kohn and L. J. Sham. *ibid.* **140**, A1133 (1965).
[8]B. I. Min and Y.-R. Jang, J. Phys.: Condens. Matter **3**, 5131 (1991).
[9]K. H. Jack, Proc. R. Soc. London Ser. A **208**, 216 (1951); P. Villars and L. D. Calvert, *Pearson's Handbook of Crytallographic Data for Intermetallic Phases* (Americal Society for Metals, Metals Park, OH, 1985).
[10]B. I. Min (unpublished).
[11]B. I. Min. T. Oguchi, H. J. F. Jansen, and A. J. Freeman, J. Magn. Magn. Mater. **54-57**, 1091 (1986); S. C. Hong, J. I. Lee, and A. J. Freeman, *ibid.* **99**, L45 (1991).
[12]S. Ohnishi, A. J. Freeman, and M. Weinert, Phys. Rev. B **28**, 6741 (1983); C. L. Fu and A. J. Freeman, *ibid.* **33**, 1755 (1986).

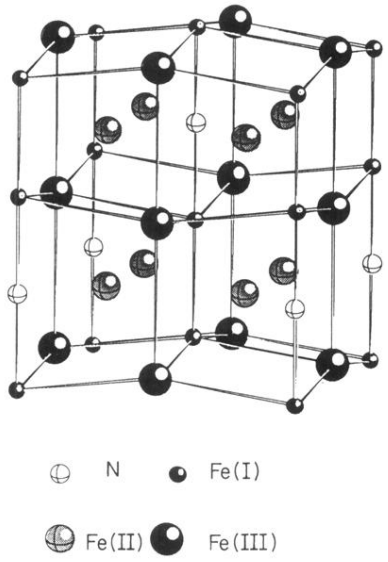

FIG. 1. Crystal structure of $Fe_{16}N_2$.

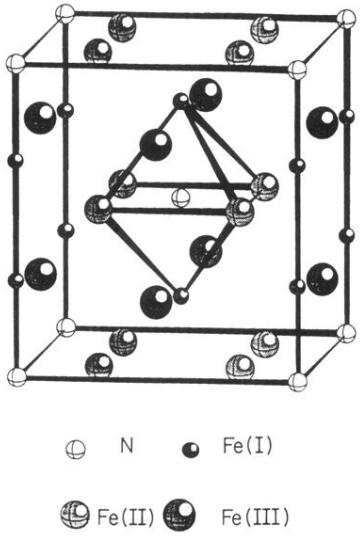

FIG. 2. Body-centered tetragonal (bct) unit cell of $Fe_{16}N_2$. Lattice constants of the a and c axes are 5.72 and 6.29 Å, respectively.